

# Effects of $\text{TiO}_2$ brookite nanoparticles size and homogeneity on photocatalytic degradation of Perfluorooctanoic Acid

Lorelei Dippy  
Department of Chemistry and Biochemistry  
The University of North Carolina Asheville  
One University Heights  
Asheville, North Carolina 28804 USA

Faculty Advisor: Dr. Oksana Love

# Abstract

Perfluorooctanoic Acid (PFOA), a type of per- and polyfluoroalkyl substance (PFAS), is an environmentally persistent and highly stable organic pollutant. Both the industrial use of PFOA prior to the early 2000's and ineffective water treatments for PFAS have resulted in the contamination of drinking water sources. Photocatalysis is a diverse degradation method utilizing light for the formation of reactive oxidative species capable of targeting and breaking PFOA's C-C and C-F bonds. Titanium Dioxide,  $\text{TiO}_2$ , is an abundant photocatalyst with three crystalline polymorphs: anatase, rutile, and brookite. Due to the previous difficulty in synthesis, brookite has limited research in photocatalytic applications. Smaller size and greater surface area of  $\text{TiO}_2$  nanoparticles (NPs) can increase photocatalytic lifespan as well as rate of degradation. Commercially purchased and synthesized  $\text{TiO}_2$  NPs differ in size and homogeneity, therefore a comparison study was conducted to determine their effects on PFOA degradation. Purchased brookite with a degradation of PFOA at 44% out-performed synthesized brookite samples made from a synthetic route "Method 1". A newer method of hydrothermal synthesis, "Method 2", resulted in particles with unique shape and size distribution that show promise for degradation.

## 1. Introduction

With the progression of modern technology, there has been a movement to understand and investigate the use of certain chemicals meant for industrial manufacturing, as well as develop new technologies towards proper disposal of such substances. This holds true in the U.S. as Per- and Polyfluorinated Substances, also known as PFAS, have become an ever-growing concern, even with a decline in their use nationally since the early 2000s<sup>1</sup>. PFAS is the all-inclusive name covering a multitude of chemicals that have been incorporated into products ranging from adhesives, cosmetics, and pesticides, to non-stick cooking ware, fire-fighting foams, and paints.<sup>1,2</sup> Their stability, ability to repel oil and water, and low reactivity are what make them a truly multi-purpose group of chemicals, allowing for a plethora of uses even outside the aforementioned products, many of which are still needed and consumed in the U.S. frequently.<sup>1,2</sup> Though PFAS contamination occurs in air, soil, and water, they have been found in the bloodstreams of both humans and animals.<sup>1,2,3</sup> Kotlarz, Nadine, et al. ran a study that detected two commonly found legacy PFAS, Perfluorooctane sulfonic acid (PFOS) and Perfluorooctanoic Acid (PFOA),

in the water of the Cape Fear River and consequently, in the bloodstreams of Wilmington inhabitants in the surrounding area.<sup>4</sup> In the City of Asheville, PFAS have been found in trace amounts within water bodies such as the French Broad River and Mills River after a 2019 study was conducted by Duke University and UNC Chapel Hill.<sup>5</sup> Since the initial study, the City of Asheville takes annual source and treated water samples for detectable PFAS compounds.<sup>5</sup>

Alongside uncertain and unpredictable impacts in contaminated ecosystems, long term PFAS exposure leads to accumulation in the human body that can be traced to health risks including, but not limited to, kidney cancer, testicular cancer, heightened infertility, thyroid disease, and risk of miscarriage and pregnancy-induced hypertension.<sup>3,6,7</sup>

The low reactivity and environmental longevity of PFAS like PFOA is caused by the overall structure of the compounds, which consists of a carbon chain with strong, high energy C-F bonds rather than C-H bonds, and overall low polarity.<sup>3,6</sup> Long-chain PFAs are generally labeled such if a molecule within the perfluoroalkyl carboxylic acid (PFCA) subgroup, such as PFOA, contains eight or more carbons if within the perfluoroalkyl sulfonic acid (PFSA) subgroup contains six or more, while the newer alternative short-chain PFAS are the smaller counterparts in respect to each subgroup (see figure 1).<sup>3</sup>

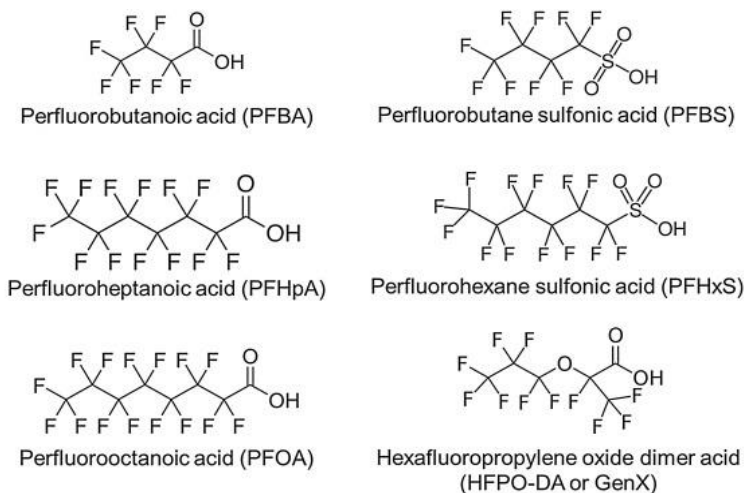


**Figure 1:** Structures of common legacy perfluoroalkyl substances (PFAS) and replacement PFAS.<sup>4</sup>

Many long-chain PFAS have limited regulation, with restrictions being imposed to keep their numbers out of excess. The World Health Organization, WHO, set a standard for a PFAS limit in its Drinking Water Directive Proposal in 2018, setting an advised limit of 0.5 µg/L of total PFAS in water as well as a 0.1 µg/L limit for a singular type of PFAS compound.<sup>3</sup> The most recent and lowest advisory level is currently for PFOA, at 4.0 parts per trillion, making its prevalence a concerning hazard.<sup>8</sup>

The research for finding methods to manage PFOA contamination through removal or degradation is still ongoing, with various techniques being developed that have greater success with certain PFAS subgroups or specific PFAS compounds themselves. Conventional methods often used in water treatment plants such as aquatic aerobic and anaerobic treatments, UV irradiation, and photolysis don't have as substantial PFAS degradation resulting from the inability to break down the C-F bonds.<sup>3,9</sup> In the field, existing methods currently known that have more success in PFAS decontamination include adsorption, anion exchange processes, plasma treatments, and photocatalysis.<sup>3,10</sup> The best adsorption implemented for PFAS is the utilization of hydrophobic and electrostatic attractions to create attachments between the adsorbent of choice and the target PFAS molecules, with anion exchange resins used in the same manner via ionic attractions, particularly from the anionic end tail.<sup>3,10</sup> Plasma treatment is an advanced oxidation method in which plasma is introduced to water through technological means, generating oxygen species such as OH radicals and  $O_2^-$  radicals, which can then chemically degrade organic pollutants, as shown in Figure 2.<sup>9,11</sup>

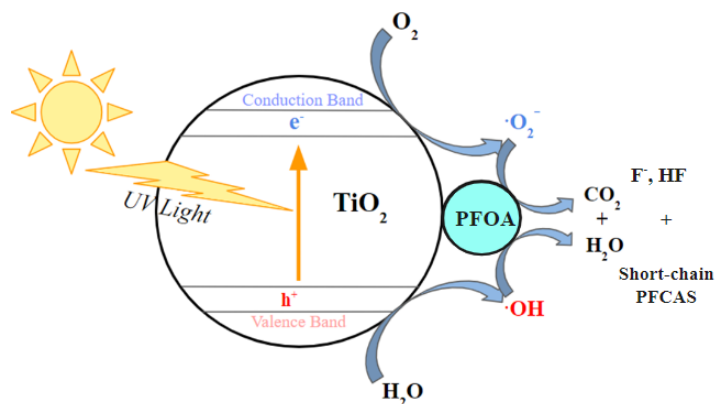


**Figure 2:** Photocatalysis of PFAS general scheme, courtesy of Victoria Magyar.

Photocatalysis as an oxidative process alternative to plasma treatments has shown promising results in the degradation of varying PFAS compounds. Unlike previously mentioned methods that solely utilize PFAS removal from water sources, photocatalysis is energetically favorable in its degradation of PFAS, long and short chained, with a variety of photocatalyst options, of which there are opportunities for them to be implemented into infrastructure or dispersed in solution.<sup>9</sup>

This study will focus on a particular photocatalyst with known abilities regarding light induced degradation. As a photocatalyst, Titanium Dioxide,  $TiO_2$ , has the capabilities of degrading pollutants and volatile organic compounds under the preference of UV or while still being nontoxic, stable, and a good semiconductor material.<sup>12</sup> The  $TiO_2$  photocatalyst was investigated by Chowdhury, Nusrat, *et al.* as a degrading agent for select PFAS. From the study it was observed that  $TiO_2$ , along with sulfur radicals generated by persulfate or sulfite, were able to chemically decompose specific long chain perfluoroalkyl carboxylic acids (PFCAs), a type of long chain PFAS, with success, as well as short-chain 6:2 Fluorotelomer Sulfonate (FTS)<sup>7</sup>. Dillert, Ralf, *et al.* used UV photocatalysis with  $TiO_2$  and phosphotungstic acid for the degradation of

certain PFCAs, yielding relatively small but observable efficiencies to lay the groundwork for future research, and has increased the PFCA degradation compared to without the photocatalyst.<sup>13</sup>

Titanium Dioxide, as a promising photocatalyst, would need the right conditions to be able to properly degrade specific PFAS subgroups and specific compounds. PFOA specifically has shown favorable photodegradation outcomes under lower pH and oxygen-rich conditions.<sup>14, 15</sup> The properties of  $\text{TiO}_2$  itself matter greatly for the efficiency and success rate of photocatalytic degradation.  $\text{TiO}_2$  groupings in nanoparticles exist as three crystal polymorphs: brookite which will be the target polymorph of this study, Anatase, and Rutile, all of which are stable, though have the ability to undergo phase transformations.<sup>12,14,17</sup> Figure 4 shows a general lattice structure for each polymorph.

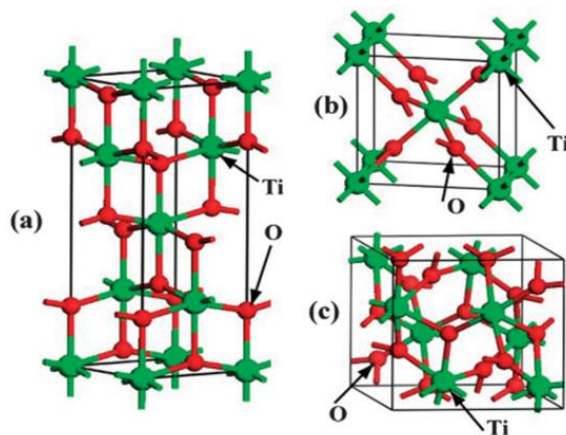


**Figure 3:** The conventional cells for anatase (a), rutile (b) and brookite (c)  $\text{TiO}_2$ . The big green spheres represent Ti atoms, and the small red spheres represent O atoms.<sup>12</sup>

Out of the three polymorphs, Orthorhombic brookite lacked the most research due to past difficulty of synthesis, however now brookite has been observed to be stable and shows significant promise as a photocatalyst due to its wide bandgap between 3.1-3.4 and higher photocatalytic activity in a pure phase with high surface energy; the {210} facet of brookite is recognized by high reactivity, similar to the 101 face of anatase.<sup>18</sup> This variety of bandgaps is in an ideal range for UV light. Figure 4 shows a difference in polymorph XRD phases, each with distinguishable peaks. Specific peaks, depending on the  $2\theta$  angle of incidence where intensity spikes, represents a 3-digit lattice plane orientation (Miller indices) – the spectra containing these peaks on a large  $2\theta$  range represent each distinguishable  $\text{TiO}_2$  crystal polymorph diffraction pattern.

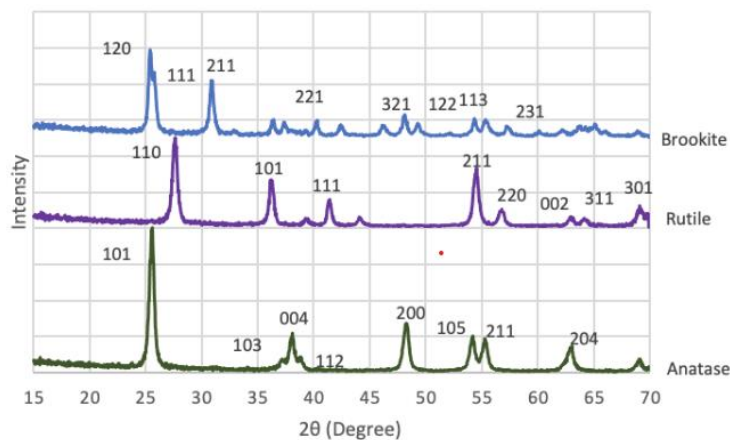


**Figure 4:** XRD Patterns of Purchased Anatase, Rutile, and Brookite.<sup>20</sup>

Current research has allowed for brookite to become more popular, allowing for a continual progression of altered synthetic routes. Though phase transition instability is an area of concern for Brookite, factors such as pH, temperature, and surface area are able to improve stability, and create specific formations of Brookite with differing sizes and possibly different levels of photocatalytic activity, such as nanosheets, nanocubes, or nanoflowers<sup>17,18,19</sup>. Kandiel, Tarek A., et al. observed synergies between Anatase and Brookite from higher photocatalytic activity, with pure-phase Brookite showing the greatest amount of catalytic activity.<sup>19</sup>

The comparison of purchased and hydrothermally synthesized gives a better look into the nuances among the shape and size variation of TiO<sub>2</sub> brookite alone. Through a facile thermal synthesis, it would be expected to see possible larger sizes for particles, even if surface area may be greater depending on their specific shape and surface.

## 2. Experimental Methods

### 2.1: Materials

Pure phase brookite nanocrystals were used as-purchased from Sigma Aldrich. Titanium Oxysulfate Hydrate – Sulfuric Acid (TiSO<sub>4</sub>•xH<sub>2</sub>O) was purchased from Alfa Aesar. PFOA (solid) was purchased from VWR. C<sup>13</sup>-PFOA Isotopic Internal standard and 96% C<sup>12</sup> PFOA was purchased from Wellington Labs

## 2.2: Safety

Caution should be taken when conducting experimental synthesis of TiO<sub>2</sub> brookite, particularly regarding the use of acids. NoChromix is a strong oxidizer when mixed with sulfuric acid for glass cleaning. Take caution when handling NoChromix, as it causes harm upon ingestion and eye exposure, and can irritate upon skin contact and inhalation. Gloves and safety splash goggle should always be worn when working with NoChromix.<sup>21</sup>

Caution should also be taken when using Hydrochloric Acid (HCl). HCl is very corrosive, has high toxicity, and can cause severe damage to organs, skin, and eyes. Hydrogen chloride gases can also pose a health risk upon inhalation. It is necessary to always wear splash goggles and gloves when working with HCl, as well as always handling HCl under a fume hood.<sup>22</sup>

Solid TiO<sub>2</sub> has few acute hazards, and though it is not a known eye or skin irritant, it is best to avoid inhalation of particles, as well as allowing contact with skin, and oral consumption. TiO<sub>2</sub> should be stored in a dry location at room temperature or below. Goggles and gloves should still be worn when working with solid TiO<sub>2</sub> nanoparticles.<sup>23</sup>

PFOA in solution (methanol) is highly flammable and is greatly toxic upon inhalation. It is not only possibly carcinogenic but may also cause fertility issues and organ damage upon invasive exposure. Because methanol is highly volatile, gloves and splash goggles should always be worn when handling the PFOA solutions. PFOA in methanol should be handled under a fume hood.<sup>24</sup>

## 2.3: Synthesis of particles

**Method 1:** 2.5 grams of Titanium Oxysulfate Hydrate precursor (TiSO<sub>4</sub>·xH<sub>2</sub>O) were added to 50 mL DI Water. The precursor solution was stirred until clear, and 25 mL of 0.21M NaOH was added, forming a white precipitate. While the solution stirred, concentrated NaOH was added dropwise to the mixture to increase precipitation and bring the initial solution pH to 12.5. The resulting gel-precipitate was then washed via centrifugation at 5000 rpm for 10 minutes and decanted with DI water three separate times. Concentrated NaOH was used again to bring the final pH back to 12.5. Solutions were put into polyphenylene polymer (ppl)-lined autoclaves inside a steel autoclave and placed inside a muffle furnace. All samples were heated to 220°C with reaction times at 21 and 24 hours. Thermally treated samples were centrifuged 3 times for 20 minutes and decanted three times. Samples were oven-dried and ground for SEM and XRD analysis. Figure 5 shows a visual scheme of the synthetic route.

**Method 2:** 1.19 grams of TiSO<sub>4</sub>·xH<sub>2</sub>O was stirred into 25 mL of DI water until clear. 50 mL of 0.5 M NaOH was added to the 25 mL of precursor solution to form a precipitate with an initial pH of 12.5, with no concentrated NaOH needed. The resulting gel-precipitate was then washed via centrifugation at 5000 rpm for 10 minutes and decanted with DI water three separate times. Similar to Method 1, Concentrated NaOH was used again to bring the final pH back to 12.5. Solutions were put into

polyphenylene polymer (ppl)-lined autoclaves inside a steel autoclave and placed inside a muffle furnace. All samples were heated to 220°C with reaction time of 24 hours. Thermally treated samples were centrifuged 3 times for 20 minutes and decanted three times. Samples were oven-dried and ground for SEM and XRD analysis. Figure 5 shows a visual scheme of both synthetic routes.

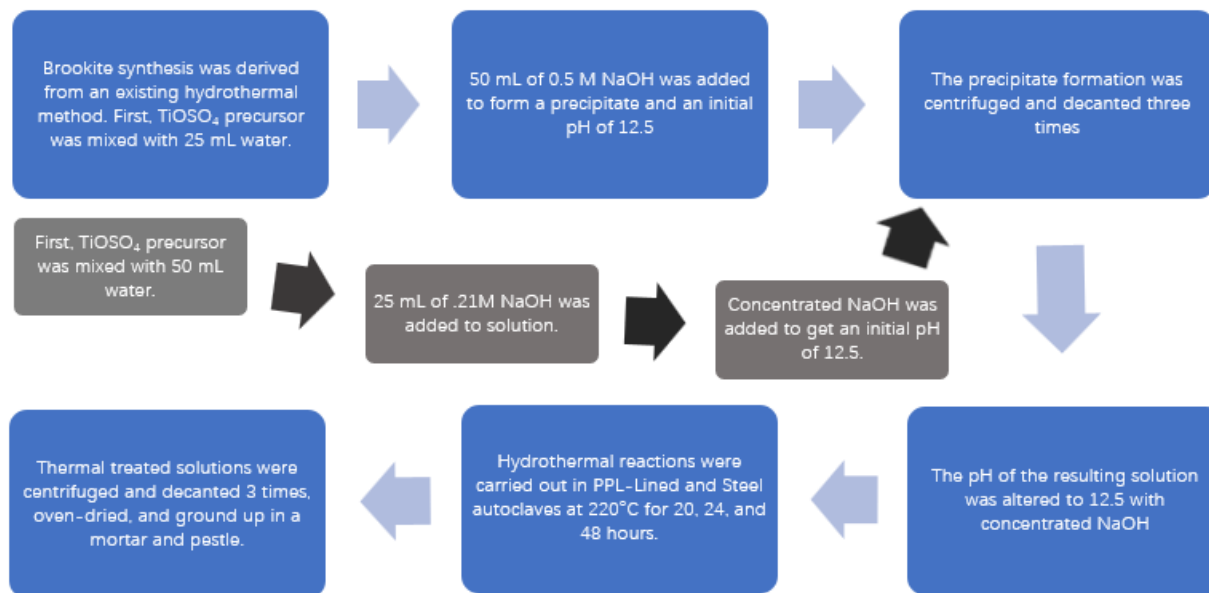


**Figure 5:** Hydrothermal brookite Method 2 (blue) and Method 1 (grey) synthesis steps

## 2.4: Characterization

Purchased and synthesized NPs were characterized using a Bruker D2 Phaser Benchtop X-Ray Diffractometer and a Jeol JSM-IT700HR SEM. XRD was used for phase identification via comparison to an embedded crystal phase references courtesy of the Crystal Open Database. Photodegradation trials occurred inside a Rayonet reactor (12W, 254nm). Photodegradation analysis was conducted using a Shimadzu 8040 Liquid Chromatography Tandem Mass Spectrophotometer with a C18 Phenomenex reverse-phase column.

## 2.5: Calibration Curve

All PFOA standard solutions were made using 80:20 H<sub>2</sub>O:MeOH solvents. A calibration curve was developed using vials containing 390 µL of PFOA standards in solution and 10 µL of 1000 ppb isotopic internal standard, with concentration of calibration points ranging 0.5, 1.0, 5.0, 10, 25, 50, 100 ppb. All standards were diluted from a 96% PFOA 2000 ppb solution. The LOD was measured at 6.312 ppb and LOQ at

19.13 ppb, with an  $R^2$  value of 0.9772. An ideal  $R^2$  reaches values even higher with the improvement of running more 100ppb standards. The LOQ is higher than the 10ppb, however it is not above the value of any data points, therefore making all data valid.

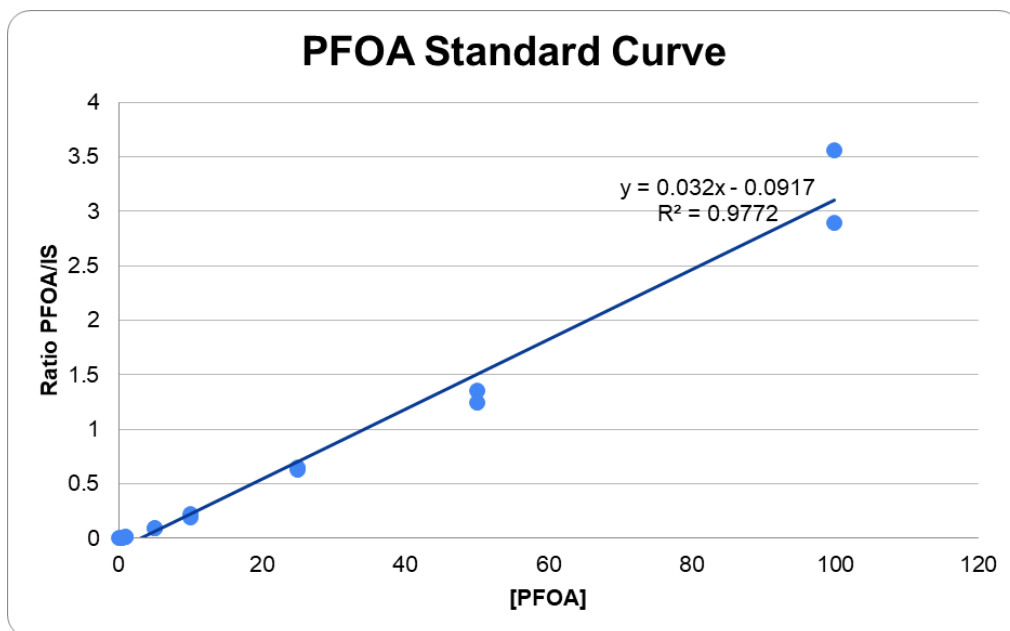


**Figure 6:** PFOA Calibration Curve. LOD = 6.312 ppb LOQ = 19.13 ppb.

## 2.6: PFOA Degradation

. Photocatalysis samples were contained as a 60 ppb PFOA solution in 80:20 water: acetonitrile solvent in a quartz tube. The pH was kept unaltered. Afterwards, 6.0 mg of Brookite were added to every tube, and left in darkness under cold conditions to equilibrate. All photocatalysis runs were performed UV reactor for two total hours of UV irradiation. An initial 1.0 mL was collected from the tubes, followed by samples taken every 30 minutes during irradiation. Brookite NPs were centrifuged out at 10,000 RPM for 15 minutes. Subsequently 500  $\mu$ L were collected via syringe from the microcentrifuge tubes and syringe-filtered out into a separate vial. A 0.3  $\mu$ m polyvinyl difluoride (PVDF) filter was used for syringe filtration. From the separate vial, 390  $\mu$ L of solution were pipetted from each vial into labeled, corresponding LC vials. 10  $\mu$ L of internal standard were added to each LC vial.

## 3. Results and Discussion

### 3.1: Characterization of brookite TiO<sub>2</sub> NPs

Both particles resulting from the Method 2 synthesis and the Method 1 synthesis were characterized under SEM and XRD. Table 1 shows the differences in surface and size as both the synthesis method changes along with thermal treatment times. For the synthesis Method 1, NPs had a “hop”-shape, with slightly amorphous nature shown by a flaky and fragmented surface. For the 21-hour synthesis, particles had both less shape homogeneity and exaggerated amorphousness with some particles forming a clumped, agglomerated appearance. Measurements are shown along the particles in nm and  $\mu\text{m}$  where necessary. All particles follow XRD diffraction patterns with both reference lines for brookite standards, as well as following the same diffraction pattern as purchased brookite itself (Figure 8 a-d).

The hop-like NPs for the 21 hour thermally treated samples from Method 1 synthesis had an average length range of 450-550nm, while the diameter was on average 100-150nm (Figure 7 A-C). For the 24 hour thermally treated NPs under Method 1, average length range was 500-650nm, while average diameter range was around 170-250nm (Figure 7 D-F). For the first 24 hour thermally treated samples under Method 2, particles formed large aggregates on the microscale, ranging from 1.0-1.5  $\mu\text{m}$  in at least one diameter on average (Figure 7 G-I). These aggregates however are composed of much smaller scale nanoparticles, which appear spindled and curved like rings. In length these rings had a variety of lengths, many of which averaged around 300-400nm. The thickness of these spindles averaged around 30-60 nm (Figure 7 G-I).

The second 24-hour thermally treated sample from Method 2 appeared to be more amorphous than the previous sample, attributed to slightly lower drying time and possibly escaping of supernatant from the autoclave under pressure and heat (Figure 7 J-L). The presence of agglomerates and aggregates with TiO<sub>2</sub> spindles show a low homogeneity in both size and shape overall (Figure 7 J-L). The spindles, however, retain the same characteristics as the more crystalline sample under Method 2, with ring lengths around 260-380nm and thickness ranging from 30-60nm. The purchased brookite follows a similar trend of large microscale aggregates around 2-3µm. The aggregates are made up of small NPs with no defined shape and average lengths in at least one diameter of 80-120nm (Figure 7 M-N).

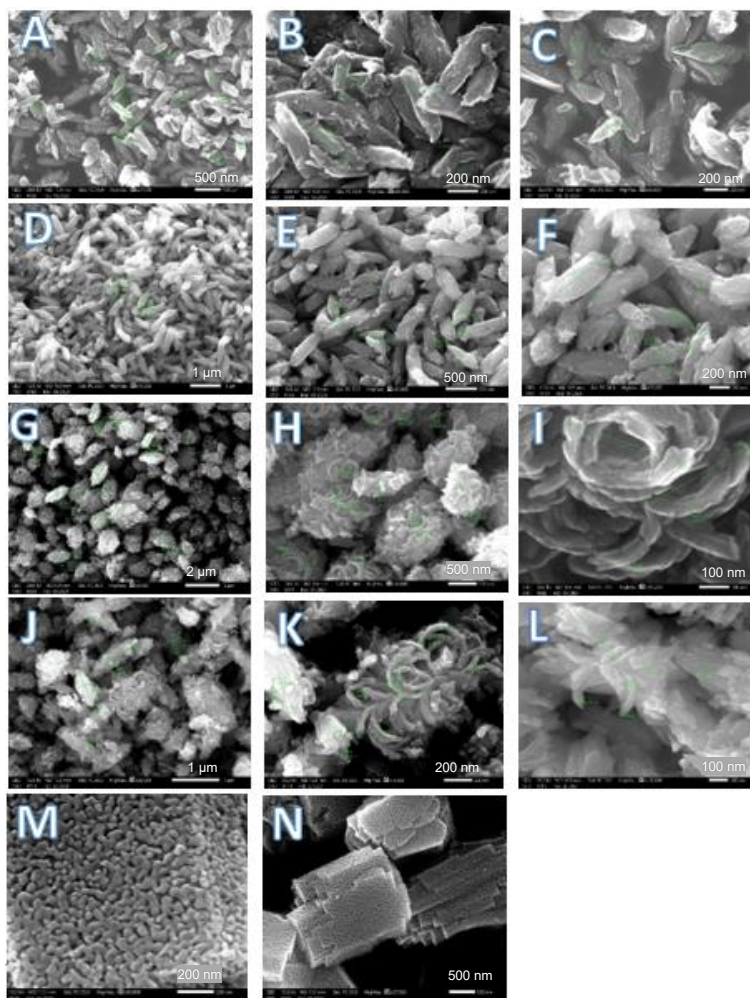


**Figure 7:** SEM images with digital measurements, in green, for (A-C) 21 hour Method 1 brookite, (D-F), 24 hour Method 1 synthesized brookite, (G-I) 24 hour Method 2 synthesized brookite, (J-L) Second 24 hour Method 2 synthesized brookite, (M-N) purchased brookite. Scale bars are shown in the bottom right.

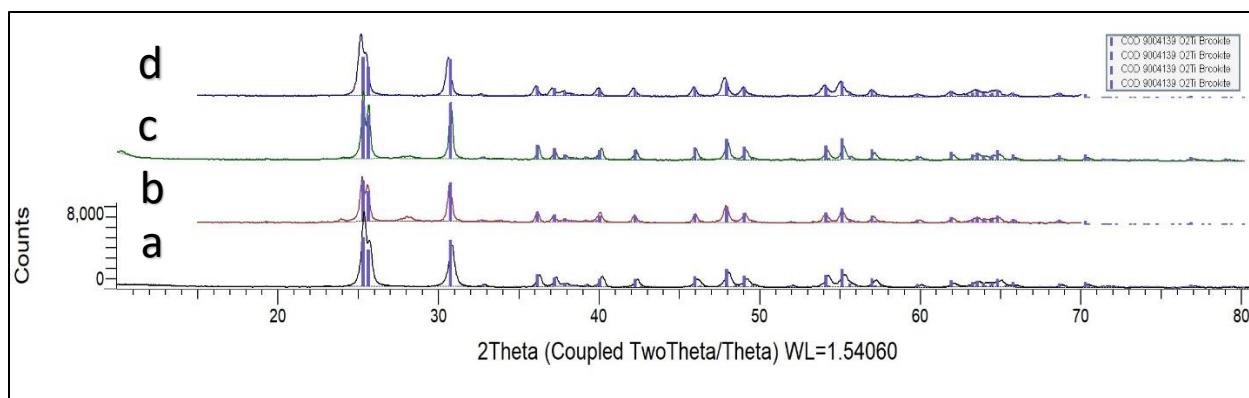


**Figure 8:** XRD spectra for  $\text{TiO}_2$  samples including (a) purchased brookite [COD 9004139 brookite], (b) Method 1 brookite at 21 hours [COD 9004139 brookite], (c) Method 1 brookite at 24 hours [COD 9004139 brookite], (d) Method 2 synthesized brookite at 24 hours [COD 9004139 brookite]. The second Method 2 synthesized brookite samples at 24 hours was assumed to have brookite diffraction patterns.

### 3.2: Photocatalytic performance of purchased and synthesized brookite $\text{TiO}_2$

Resulting LCMS-MS sample curve area/IS curve area ratios were calculated and plugged into the calibration curve to find resulting the concentration. The initial measured concentration of the sample was used as the 100% value, and all percentages of PFOA in solution were compared to the initial.

Purchased brookite NPs and brookite synthesized under Method 1 were employed in photocatalysis trials. The trial for 24-hour brookite was run once ( $n=1$ ), while 21-hour brookite and purchased brookite were run twice ( $n=2$ ) (Figure 9). Purchased brookite and the second Method 2 brookite sample performed the best and was able to degrade PFOA by 44% (Figure 9). The first Method 2 brookite sample had been able to degrade PFOA by 24% (Figure 9). The 21-hour older synthesis brookite NPs degraded PFOA by 29%, while the 24-hour older synthesis brookite NPs were only to degrade PFOA by 5% (Figure 9). The dip in PFOA percentage values for the 24-hour Method 1 brookite may reveal a better picture of brookite synthesis if repeated in trials compared to the final value at 120 minutes of UV irradiation (Figure 9).

The 44% removal of PFOA from both purchased brookite and the second Method-2 derived brookite can be attributed to how surface and shaping of the sample particles differ from their counterparts. Purchased Brookite, though made up of microscale aggregates, consists of a sponge-like surface with small, randomly shaped nanoparticles that differ in size but remain small ( $<80\text{nm}$ ). The grooves in purchased brookite samples resemble more porous nanoparticles. This could allow for better adsorption of PFOA, as well as greater coverage of light on the surface, as well as further light penetration. This pattern can be seen in the second Method-2 derived brookite. Aggregates from this sample had a similar general size, with small particles ( $<60\text{nm}$ ) protruding off the surface. These particles do not appear to be as sponge-like

as the purchased brookite, however the benefit of Method-2 brookite spindles should be the same as having the grooves in purchased samples.

The first sample of brookite synthesized from Method 2 also has spindles, however worse performance can be attributed to much larger aggregates, and longer spindles which take up more space. Both 24- and 21-hour brookite particles synthesized from Method 1 were larger overall compared to the spindles and oblong-amorphous particles on the purchased brookite surface. This contributes to worse performance, as larger size results in a decreased amount of surface area. The greater shape and size homogeneity of these particles decreases the chance of smaller particles being present in the sample.

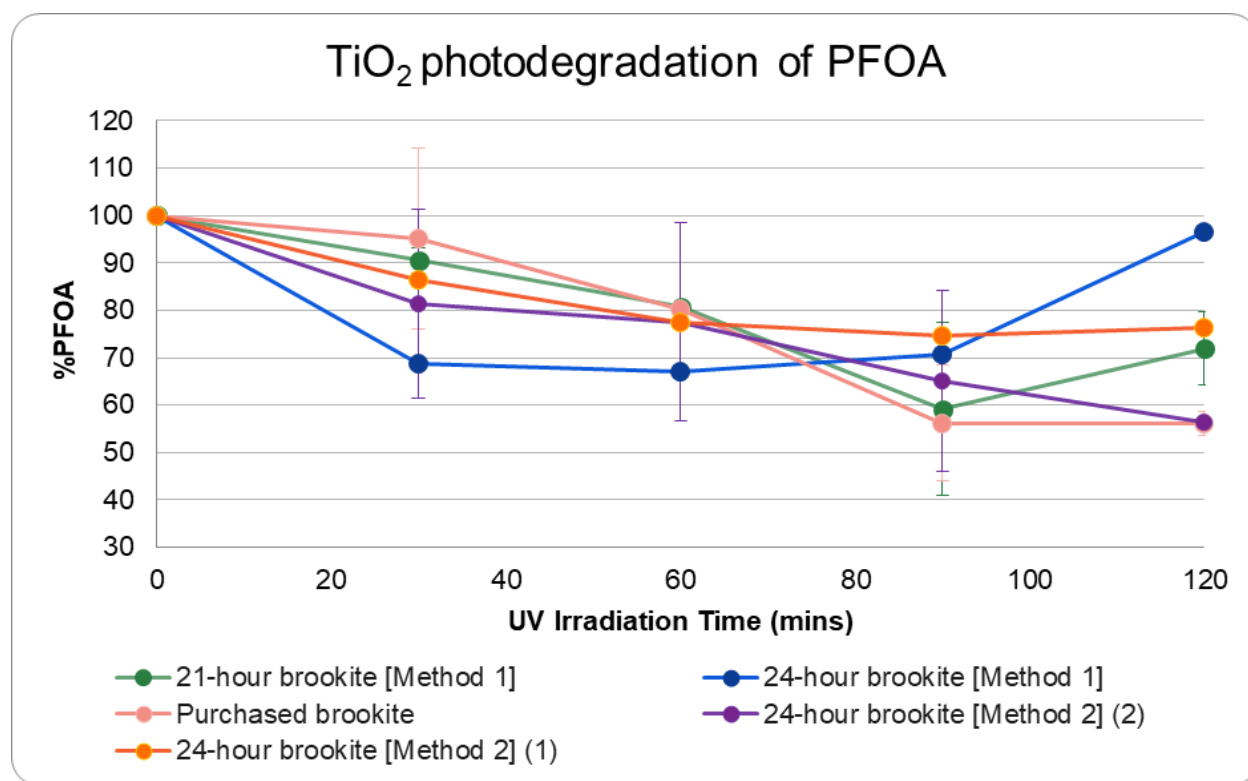


**Figure 9:** Plot comparing the degradation of PFOA under UV Irradiation with varying photocatalyst types.

## 4. Conclusion and Further Research

Purchased brookite NPs were observed to have formed large, rough-surfaced aggregates which were on the microscale. The individual nanoparticles were not homogenous in shape or size, though the larger aggregates had relatively greater homogeneity. All Method 1 NPs formed a hop-like shape after thermal treatment, centrifugation, and drying. Method 2 NPs, though both run for 24 hours, have formed what appear to be nanoflowers with curly/curved rings protruding from the center. Method 2 NPs had smaller individual particles similar to purchased brookite.

Under photodegradation trials, purchased brookite and 24-hour brookite [Method 2] (2) performed the best, while 24-hour Method 1 brookite performed the worst. At a pH of 7, the increase in amorphousness in the 24-hour Method 1 brookite appears to have greatly impacted its final degradation of PFOA, even if it had slightly smaller particles. It would be in the best interest to continue testing these specific particles to determine accurate performance. The greater performance of purchased brookite could be attributed to the ability of smaller NPs forming the aggregates to have a greater surface area compared to other synthesized NPs, as well as having a higher crystallinity. This could mean that synthesized brookite using Method 2 may have promising results for degradation.

Preliminary studies and data still have room for further method development. The synthesis of brookite nanoparticles has currently been focused on high pHs and long reaction times. Amorphousness appears to increase as times for thermal treatment/reaction decreases rather than particle agglomeration being prevented with a remaining particle smoothness. A future step for the benefit of understanding the effect of nanoparticle surface, shape, and size on degradation is to look at the effect of photocatalysis and possible HF production on the particles themselves. This would be done via a second post-irradiation characterization. It is an area of interest to change the method of filtration, particularly switching from PVDF filters, change to using an isotopic standard for decomposition products of PFOA, and begin doping  $\text{TiO}_2$  to further observe what facets of brookite NPs matter most when conducting photodegradation trials. Increasing number of trials per sample will be able to further solidify the photocatalytic performance of the varying photocatalyst types employed in the trials.

## Acknowledgements

I would like to thank Dr. Oksana Love, Luca Antonescu, Luke Coward, the University of North Carolina at Asheville Department of Chemistry and Biochemistry, NSF Grant S-STEM #1833604, Dr. Melanie Heying, and the fantastic members of the Love Lab!

## References

- 1) *PFAS Chemicals Overview* | ATSDR. 9 Sept. 2022, <https://www.atsdr.cdc.gov/pfas/health-effects/overview.html>.
- 2) Glüge, Juliane, et al. "An Overview of the Uses of Per- and Polyfluoroalkyl Substances (PFAS)." *Environmental Science: Processes & Impacts*, vol. 22, no. 12, 2020, pp. 2345–73. [pubs.rsc.org](https://pubs.rsc.org), <https://doi.org/10.1039/D0EM00291G>.
- 3) Gagliano, Erica, et al. "Removal of Poly- and Perfluoroalkyl Substances (PFAS) from Water by Adsorption: Role of PFAS Chain Length, Effect of Organic Matter and Challenges in Adsorbent Regeneration." *Water Research*, vol. 171, Mar. 2020, p. 115381. ScienceDirect, <https://doi.org/10.1016/j.watres.2019.115381>.
- 4) Kotlarz, Nadine, et al. "Measurement of Novel, Drinking Water-Associated PFAS in Blood from Adults and Children in Wilmington, North Carolina." *Environmental Health Perspectives*, vol. 128, no. 7, p. 077005. [ehp.niehs.nih.gov](http://ehp.niehs.nih.gov) (Atypon), <https://doi.org/10.1289/EHP6837>.
- 5) *PFAS Mitigation Efforts*. The City of Asheville. <https://www.ashevillenc.gov/departments/water/pfas-mitigation-efforts/>
- 6) Blake, B. E.; Fenton, S. E. Early Life Exposure to Per- and Polyfluoroalkyl Substances (PFAS) and Latent Health Outcomes: A Review Including the Placenta as a Target Tissue and Possible Driver of Peri- and Postnatal Effects. *Toxicology* 2020, 443, 152565.
- 7) Chowdhury, Nusrat, et al. "Dependency of the Photocatalytic and Photochemical Decomposition of Per- and Polyfluoroalkyl Substances (PFAS) on Their Chain Lengths, Functional Groups, and Structural Properties." *Water Science and Technology*, vol. 84, no. 12, Dec. 2021, pp. 3738–54. <https://doi.org/10.2166/wst.2021.458>.
- 8) US EPA, O. Per- and Polyfluoroalkyl Substances (PFAS).
- 9) Paul Guin, Jhimli, et al. "Challenges Facing Sustainable Visible Light Induced Degradation of Poly- and Perfluoroalkyls (PFA) in Water: A Critical Review." *ACS Engineering Au*, vol. 2, no. 3, June 2022, pp. 134–50.
- 10) Chowdhury, Nusrat, et al. "Dependency of the Photocatalytic and Photochemical Decomposition of Per- and Polyfluoroalkyl Substances (PFAS) on Their Chain Lengths, Functional Groups, and Structural Properties." *Water Science and Technology*, vol. 84, no. 12, Dec. 2021, pp. 3738–54. <https://doi.org/10.2166/wst.2021.458>.

- 11) Shaw, Priyanka, et al. "Bacterial Inactivation by Plasma Treated Water Enhanced by Reactive Nitrogen Species." *Scientific Reports*, vol. 8, no. 1, July 2018, p. 11268. [www.nature.com](http://www.nature.com), <https://doi.org/10.1038/s41598-018-29549-6>.
- 12) Zhang, Jinfeng, et al. "New Understanding of the Difference of Photocatalytic Activity among Anatase, Rutile and Brookite TiO<sub>2</sub>." *Physical Chemistry Chemical Physics*, vol. 16, no. 38, 2014, pp. 20382–86. <https://doi.org/10.1039/C4CP02201G>.
- 13) Dillert, Ralf, et al. "Light-Induced Degradation of Perfluorocarboxylic Acids in the Presence of Titanium Dioxide." *Chemosphere*, vol. 67, no. 4, Mar. 2007, pp. 785–92. ScienceDirect, <https://doi.org/10.1016/j.chemosphere.2006.10.023>.
- 14) Wang, Yuan, and Pengyi Zhang. "Photocatalytic Decomposition of Perfluorooctanoic Acid (PFOA) by TiO<sub>2</sub> in the Presence of Oxalic Acid." *Journal of Hazardous Materials*, vol. 192, no. 3, Sept. 2011, pp. 1869–75. DOI.org (Crossref), <https://doi.org/10.1016/j.jhazmat.2011.07.026>.
- 15) Wang, Yuan, and Pengyi Zhang. "Effects of PH on Photochemical Decomposition of Perfluorooctanoic Acid in Different Atmospheres by 185nm Vacuum Ultraviolet." *Journal of Environmental Sciences*, vol. 26, no. 11, Nov. 2014, pp. 2207–14. DOI.org (Crossref), <https://doi.org/10.1016/j.jes.2014.09.003>.
- 16) Xu, Jinlei, et al. "Preparation of Brookite TiO<sub>2</sub> Nanoparticles with Small Sizes and the Improved Photovoltaic Performance of Brookite-Based Dye-Sensitized Solar Cells." *Nanoscale*, vol. 8, no. 44, 2016, pp. 18771–81. DOI.org (Crossref), <https://doi.org/10.1039/C6NR07185F>
- 17) Hu, Wanbiao, et al. "High-Quality Brookite TiO<sub>2</sub> Flowers: Synthesis, Characterization, and Dielectric Performance." *Crystal Growth & Design*, vol. 9, no. 8, Aug. 2009, pp. 3676–82. DOI.org (Crossref), <https://doi.org/10.1021/cg9004032>.
- 18) Di Paola, Agatino, et al. "Brookite, the Least Known TiO<sub>2</sub> Photocatalyst." *Catalysts*, vol. 3, no. 1, Mar. 2013, pp. 36–73. [www.mdpi.com](http://www.mdpi.com), <https://doi.org/10.3390/catal3010036>.
- 19) Kandiell, Tarek A., et al. "Brookite versus Anatase TiO<sub>2</sub> Photocatalysts: Phase Transformations and Photocatalytic Activities." *Photochem. Photobiol. Sci.*, vol. 12, no. 4, 2013, pp. 602–09. DOI.org (Crossref), <https://doi.org/10.1039/C2PP25217A>.
- 20) Stynka, Nataliya. *Effects of pH and Heating Time on the Synthesis of Titanium Dioxide Nanoparticles*. The University of North Carolina Asheville, Asheville, NC, 2021.
- 21) Godax Laboratories Inc., *MATERIAL SAFETY DATA SHEET NOCHROMIX*, <https://ehslegacy.unr.edu/msdsfiles/29169.pdf>.

22) Sigma Aldrich, *SAFETY DATA SHEET SECTION 1: Identification of the Substance/Mixture and of the Company/Undertaking 1.1 Product Identifiers Product Name : Hydrochloric Acid.*

23) Sigma Aldrich, *SAFETY DATA SHEET*; 2023.  
<https://www.sigmaaldrich.com/US/en/sds/aldrich/791326>

24) Agilent, *Safety Data Sheet Acc. To OSHA HCS 1 Identification · Product Identifier · Trade Name: PFOA/PFOS Standard (1X1 ML) · Part Number: PFM-100-1 · Application of the Substance / the Mixture Reagents and Standards for Analytical Chemical Laboratory Use.*  
[https://www.agilent.com/cs/library/msds/PFM-100-1\\_NAEnglish.pdf](https://www.agilent.com/cs/library/msds/PFM-100-1_NAEnglish.pdf).